Journal of Coordination Chemistry

ISSN: 0095-8972 (Print) 1029-0389 (Online) Journal homepage: http://www.tandfonline.com/loi/gcoo20

# Interactions of nitrogen-donor bio-molecules with dinuclear platinum(II) complexes

Snežana Jovanović, Jovana Bogojeski, Marijana Petković & Živadin D. Bugarčić

**To cite this article:** Snežana Jovanović, Jovana Bogojeski, Marijana Petković & Živadin D. Bugarčić (2015) Interactions of nitrogen-donor bio-molecules with dinuclear platinum(II) complexes, Journal of Coordination Chemistry, 68:17-18, 3148-3163, DOI: 10.1080/00958972.2015.1048240

**To link to this article:** http://dx.doi.org/10.1080/00958972.2015.1048240

*Journal of Coordination Chemistry*, 2015
Vol. 68, Nos. 17–18, 3148–3163, http://dx.doi.org/10.1080/00958972.2015.1048240





# Interactions of nitrogen-donor bio-molecules with dinuclear platinum(II) complexes

SNEŽANA JOVANOVIĆ†, JOVANA BOGOJESKI†, MARIJANA PETKOVIĆ‡ and ŽIVADIN D. BUGARČIĆ*†

†Faculty of Science, Department of Chemistry, University of Kragujevac, Kragujevac, Serbia
‡Department of Physical Chemistry, Institute of Nuclear Sciences "Vinča", University of Belgrade, Belgrade, Serbia

(*Received 22 December 2014; accepted 17 March 2015*)

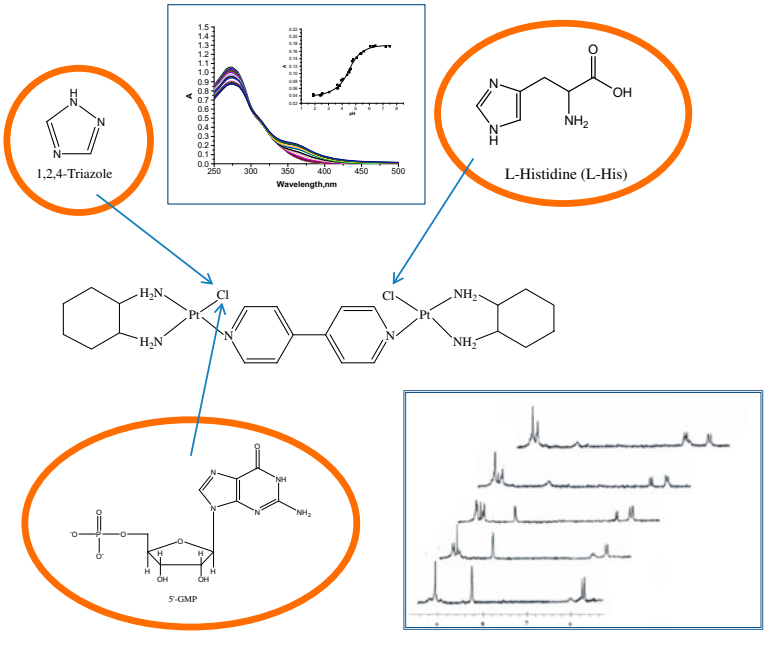


Substitution reactions of the dinuclear Pt(II) complexes, $[\{Pt(en)Cl\}_2(\mu\text{-pz})]^{2+}$ (**1**), $[\{Pt(dach)Cl\}_2(\mu\text{-pz})]^{2+}$ (**2**) and $[\{Pt(dach)Cl\}_2(\mu\text{-4,4′-bipy})]^{2+}$ (**3**), and corresponding aqua analogs with selected biologically important ligands, viz. 1,2,4-triazole, L-histidine (L-His) and guanosine-5′-monophosphate (5′-GMP) were studied under *pseudo*-first-order conditions as a function of concentration and temperature using UV–vis spectrophotometry. The reactions of the chloride complexes were followed in aqueous 25 mmol $L^{-1}$ Hepes buffer in the presence of 40 mmol $L^{-1}$ NaCl at pH 7.2,

*Corresponding author. Email: bugarcic@kg.ac.rs
Dedicated to Professor Dr Rudi van Eldik on the occasion of his 70th birthday.

whereas the reactions of the aqua complexes were studied at pH 2.5. Two consecutive reaction steps, which both depend on the nucleophile concentration, were observed in all cases. The second-order rate constants for both reaction steps indicate a decrease in the order **1** > **2** > **3** for all complexes. Also, the p$K_a$ values of all three aqua complexes were determined. The order of the reactivity of the studied ligands is 1,2,4-triazole > L-His > 5′-GMP. $^1$H NMR spectroscopy and HPLC were used to follow the substitution of chloride in the dichloride **1**, **2**, and **3** complexes by guanosine-5′-monophosphate (5′-GMP). This study shows that the inert and bridging ligands have an important influence on the reactivity of the studied complexes.

*Keywords*: Dinuclear Pt(II) complexes; Substitution; Kinetics; Reactivity



## 1. Introduction

Cisplatin is the first developed cytostatic based on a metal ion [1–3] and it is still the most used cytostatic worldwide in the treatment of different types of cancers (ovarian, head, neck, cervical, and other cancers) [1–3]. Regardless of the success of cisplatin, side-effects and resistance are the main drawbacks of this cytostatic [1–5]. A significant number of different Pt(II) complexes were synthesized with the goal to overcome the disadvantages of cisplatin [1–6].

Dinuclear and multinuclear Pt(II) complexes belong to the group of non-classical anticancer Pt(II) complexes and have a chance to overcome the drug resistance arising from cisplatin and its analogs. The multinuclear Pt(II) complex that has demonstrated the best characteristic as cytostatic is BBR3464, a trinuclear platinum complex with 1,6-hexyldiamine [7–10]. Multinuclear Pt(II) complexes form DNA adducts structurally distinct from those of cisplatin. These complexes coordinate to DNA molecule by forming cross-links that involve both strands of the DNA (interstrand cross-links) and are therefore supposed to be less sensitive to repair as both strands are affected by the damage [11, 12].

Bridging ligands play important roles in regulating the reactivity of dinuclear Pt(II) complexes by controlling the geometric symmetry, the distance between metal ions, steric and electronic features of the metal center [13–16]. Heterocyclic diazines such as pyrazine, 4,4′-bipyridine, and similar N-containing heterocycles are good bridging ligands and have an influence on the reactivity of the complexes toward nucleophiles [16–18]. These bridging ligands are π-electron acceptors and therefore are capable of accepting electron density from Pt(II), causing an increase of electrophilicity and improving the reactivity of complex toward nucleophiles [16–18].

The mechanism of interaction of bio-molecules (amino acids, peptides, proteins, fragments of DNA, enzymes) with cisplatin and structurally similar mononuclear Pt(II) complexes are well established [1–6]. The interaction of dinuclear and multinuclear Pt(II) complexes with a variety of bio-molecules is a growing field of research both *in vitro* and *in vivo*. Investigation of the kinetics and mechanism of the interactions of the dinuclear Pt(II) complexes and bio-molecules under physiological conditions give information that will improve understanding of the reactions that occur in the body when dinuclear Pt(II) complexes are used as anti-tumor drugs. Based on the obtained data, it is possible to improve the design and development of the new anti-tumor multinuclear Pt(II) complexes.

The chemistry of five-membered azole rings and their mechanism of binding to transition metal centers is also of interest to bioinorganic researchers as many important reactions in biological systems involve coordination of some form of azole to a metal. So, azole rings

readily bind with a variety of enzymes and receptors in biological systems and thus display versatile biological activities [19]. The imidazole group of L-histidine can be linked to hemeproteins that are responsible for the uptake of oxygen as well as electron transfer through cytochromes [20].

To investigate the influence of the nature of inert and bridging ligands on the reactivity of some dinuclear complexes of Pt(II), we studied the reactions of the dichloride and diaqua forms of complexes with important nitrogen-donor ligands such as 1,2,4-triazole, L-histidine, and guanosine-5′-monophosphate by using different experimental methods. The structures of the complexes and ligands are given in figures 1 and 2.



## 2. Experimental

### 2.1. *Materials*

The compounds ethylenediamine (en) (Merck), *trans*-(±)-1,2-diaminocyclohexane (dach) (Acros Organics), $K_2PtCl_4$ (Strem Chemicals), 1,2,4-triazole, L-histidine (L-His) (Merck), and guanosine-5′-monophosphate sodium salt (5′-GMP) (Acros Organics) were used without purification. The ligands pyrazine (pz) and 4,4′-bipyridine (4,4′-bipy) were also obtained from Acros Organics. $[Pt(en)Cl_2]$ and $[Pt(dach)Cl_2]$ were synthesized according to a published procedure [21], and purity of the complexes was checked by elemental

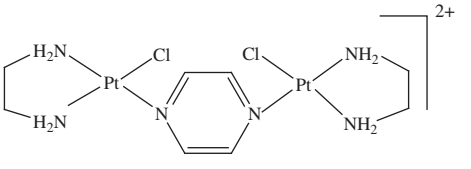


$[\{Pt(en)Cl\}_2(\mu\text{-pz})]^{2+}$, **(1)**

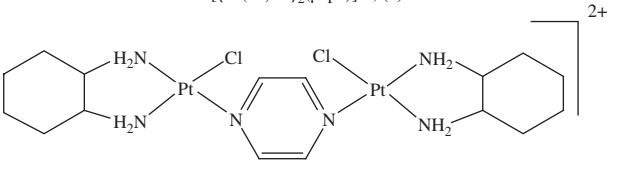


$[\{Pt(dach)Cl\}_2(\mu\text{-pz})]^{2+}$, **(2)**

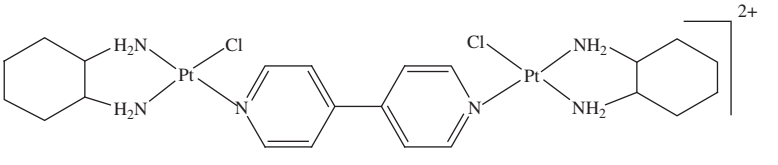


$[\{Pt(dach)Cl\}_2(\mu\text{-4,4'-bipy})]^{2+}$, **(3)**

Figure 1. The structures of the complexes.

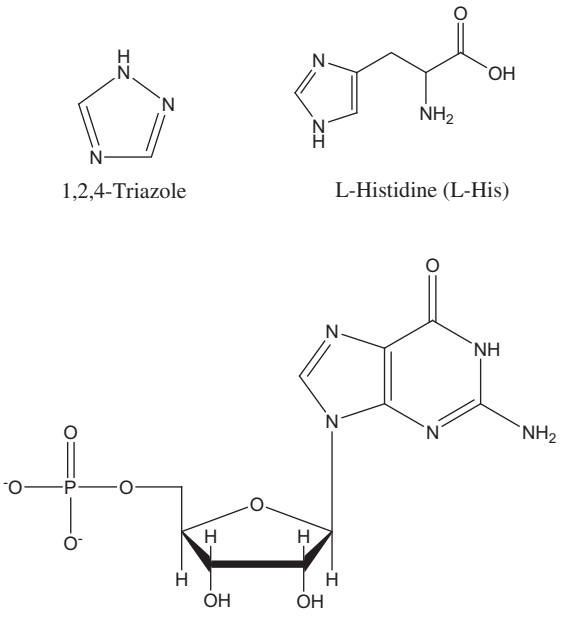


Figure 2. The structures of the ligands.



microanalyses, IR and $^1$H NMR spectroscopy. Matrix for MALDI-TOF mass spectrometry, 2,5-dihydroxybenzoic acid (DHB), and solvent for matrice and complexes (methanol) were purchased from Aldrich. Hepes buffer (N-2-hydroxyethylpiperazine-N′-2-ethanesulfonic acid), $D_2O$ (Deutero GmbH, 99.9%), dimethylformamide (DMF), and acetonitrile were also obtained from Aldrich. All other chemicals were of the highest purity available commercially. Ultrapure water was used for spectrophotometric measurements, while for HPLC water pf HPLC purity was used.

### 2.2. *Synthesis of 1, 2 and 3*

Dinuclear complexes of Pt(II), $[\{Pt(en)Cl\}_2(\mu\text{-pz})](ClO_4)_2$ (**1**), and $[\{Pt(dach)Cl\}_2(\mu\text{-pz})](ClO_4)_2$ (**2**), were prepared as described [22]. The purity of the complexes was checked by elemental microanalyses, IR, $^1$H NMR spectroscopy, and MALDI-TOF mass spectrometry.

$[\{Pt(dach)Cl\}_2(\mu\text{-}4,4'\text{-bipy})](ClO_4)_2$ (**3**) was synthesized by modification of the procedure reported in the literature [16, 22, 23] starting from $[Pt(dach)Cl_2]$. In suspension of $[Pt(dach)Cl_2]$ complex (100 mg, 0.263 mmol) in DMF (5 mL), a solution of $AgClO_4$ (53.4 mg, 0.256 mmol) in DMF (5 mL) was added. The mixture was stirred overnight in the dark at room temperature. The AgCl precipitate was removed by filtration and resulting pale yellow solution of $[Pt(dach)(dmf)Cl]ClO_4$ was used for preparation of the dinuclear platinum(II) complex.

The solution of 4,4′-bipyridine (20.5 mg, 0.131 mmol) in DMF (5 mL) was added dropwise in the solution of $[Pt(dach)(dmf)Cl]ClO_4$ and the mixture was stirred at room

temperature for 3 h in the dark. The solution was then evaporated and the residue washed with ether. A light yellow powder was obtained and left to dry in the air. Yield (81.05 mg, 59%). Anal. Calcd for [{Pt(dach)Cl}$_2$($\mu$-4,4′-bipy)](ClO$_4$)$_2$ (%): C, 25.30; H, 3.47; N, 8.05. Found: C, 25.34; H, 3.42; N, 8.08. $^1$H NMR characterization (D$_2$O, 200 MHz). $^1$H NMR (δ, ppm): 1.23–1.63 (m, dachCH$_2$, C4, C5), 1.76–2.12 (m, dach CH$_2$, C3, C6), 2.45–2.61 (m, dachCH, C1, C2), 7.92–7.98 (m, 4-pyridine, CH$_\beta$), 8.87–9.01 (m, 4-pyridine, CH$_\alpha$). IR (KBr, 4000–300 cm$^{-1}$): 3103–3450 (N–H stretch); 1655 (C=N stretch); 1090–1100 (perchlorate counter ion), 450–510 (Pt–N stretch).

[{Pt(en)Cl}$_2$($\mu$-pz)]$^{2+}$ (**1**), [{Pt(dach)Cl}$_2$($\mu$-pz)]$^{2+}$ (**2**), and [{Pt(dach)Cl}$_2$($\mu$-4,4′-bipy)]$^{2+}$ (**3**) were converted into their diaqua analogs by addition of equivalent amount of AgClO$_4$ to a solution of the dichloride complex and stirring at 323 K for 8 h as described in the literature [16]. The white precipitate (AgCl) formed was filtered off using a Millipore filtration unit and the solutions were diluted. Particular care was taken to ensure that the resulting solutions were free of Ag$^+$ and that the chloride complexes had been converted completely into the aqua species. The solution was acidified with HClO$_4$ to pH 2.0 (for determination of the p$K_a$ values) and pH 2.5 (for kinetic measurements). The ionic strength was adjusted with 0.01 mol L$^{-1}$ NaClO$_4$.

### 2.3. *Preparation of the samples for MALDI-TOF mass spectrometry*

The complexes were dissolved in methanol at 10 mmol L$^{-1}$. The solution of matrix, 2,5-DHB (0.5 mg/mL in methanol), was prepared prior to use. The following approach was used for application of the sample on the MALDI target; in the case of matrix-free approach, a small volume (0.5 μL) of solution of the complexes was applied to the 100-well gold sample plate. In matrix-assisted approach, the equal volume (0.5 μL) matrix solution was laid over the complex and left at room temperature to crystallize.

### 2.4. *Instrumentation*

UV–vis spectra were recorded on a Perkin Elmer Lamda 25 with automatic cell changer and Peltier temperature-controller and Perkin Elmer Lambda 35 double-beam spectrophotometer equipped with thermostated 1.00 cm quartz Suprasil cells. The pH measurements were recorded on a Jenway 4330 pH meter with a combined Jenway glass microelectrode that had been calibrated with standard buffer solutions of pH 4.0, 7.0, and 10.0 (Merck). The KCl solution in the reference electrode was replaced with a 3 mol L$^{-1}$ NaCl electrolyte to prevent precipitation of KClO$_4$ during use [24, 25]. MALDI-TOF mass spectra were acquired on a Voyager-DE Pro mass spectrometer equipped with a 50 Hz pulsed nitrogen laser emitting at a wavelength of 337 nm. The extraction voltage was 20 kV and all spectra were recorded under delayed extraction conditions and in linear mode. The spectra were acquired without the low-mass gate and without mass suppression and each spectrum represents an average of at least 400 single laser shots. $^1$H NMR measurements were performed on a Varian Gemini 2000, 200 MHz NMR spectrometer. HPLC results were obtained on a Shimadzu LC solution chromatograph with an SDP-M20A diode array detector. The column CC 250/4 NUCLEOSIL100-5C18 was used. Chemical analyses were performed on a Carlo Erba Elemental Analyser 1106.

### 2.5. *Determination of the p$K_a$ values of 1a, 2a, and 3a*

The p$K_a$ values of the diaqua complexes were determined by performing a spectrophotometric pH titration with NaOH in the pH range 2–10 at 298 K. The change in pH from 2 to approximately 3 was achieved by addition of known amounts of crushed pellets of NaOH, whereas for further increase in pH, NaOH solutions of different concentrations were used. After each addition of NaOH, 1 mL samples were taken from the complex solution to measure the pH. To avoid dilution effects due to the addition of the titrant, a large volume (250 mL) of the complex solution was used in the titration. After each addition of titrant, the solution was stirred and respective spectra were recorded. After pH measurements, the complex was discarded to avoid *in situ* precipitation as a chloride derivative.

### 2.6. *Kinetic measurements*

The kinetics of the substitution reactions of dichloride dinuclear **1**, **2**, and their diaqua analogs **1a**, **2a**, and **3a** with 1,2,4-triazole, L-His, and 5′-GMP were studied UV–vis spectrophotometrically. All kinetic measurements were investigated by following the change in absorbance at suitable wavelengths as a function of time at 310 K. In order to determine activation parameters, the reactions of all complexes with 5′-GMP were studied at three temperatures (288, 298, and 310 K). The working wavelengths were determined by recording the spectra of the reaction mixture from 220 to 500 nm. The reactions were initiated by mixing 0.5 mL of complex solutions with 2.5 mL of nucleophile solution in the UV–vis cuvette. Concentration of ligand solution was always large enough (at least 10-fold) to provide *pseudo*-first-order conditions. All reactions of the diaqua complexes were studied at pH 2.5 (0.01 mol $L^{-1}$ $NaClO_4$). Kinetic measurements for all dichloride complexes were investigated at pH 7.2 in 25 mmol $L^{-1}$ Hepes buffer with the addition of 40 mmol $L^{-1}$ NaCl, to suppress spontaneous hydrolysis of the dichloride complexes (figure S1, see online supplemental material at http://dx.doi.org/10.1080/00958972.2015.1048240). The observed *pseudo*-first-order rate constants, $k_{obsd}$, were calculated as the average value from three to five independent kinetic runs using the program Origin 6.1. Experimental data are reported in the Supplementa1 data, tables S1–S12.

### 2.7. *$^1$H NMR measurements*

$^1$H NMR measurements of **1**, **2**, and **3** with 5′-GMP were studied at pD 6.7 (pD = pH + 0.4) [26] on a freshly prepared sample of the reactants. Solutions (10 mmol $L^{-1}$) of the complexes and the same concentration of the ligand solution were prepared separately in 300 µL of $D_2O$, prior to the start of the experiment. The solution of the ligand was added to the solution of the complex to initiate the reaction. NMR spectra were recorded at 295 K and all chemical shifts are referenced to trimethylsilylpropionic acid. No buffer was used to prevent increased activation of the complexes due to coordination of phosphate or interfering signals in the observed peak area.

### 2.8. *HPLC measurements*

Reactions between **1**, **2**, and **3** (10 mmol $L^{-1}$) and 5′-GMP (20 mmol $L^{-1}$) were also investigated by reversed-phase HPLC using a column CC 250/4 NUCLEOSIL100-5C18 and an isocratic method with water as a mobile phase, flow: 1 mL $min^{-1}$. The calibration of

the system was done with acetonitrile and water, in different ratios, starting from MeCN : $H_2O$ = 100% : 0%. The calibration is finished when only water flows through the column. For each reaction, the solutions of the complex and the ligand were prepared in 25 mmol $L^{-1}$ Hepes buffer with 40 mmol $L^{-1}$ NaCl, they were mixed and kept in a thermoblocker at 310 K during all reaction time. At defined time intervals, a sample of reaction mixture (20 μL) was injected into the column and chromatograms were recorded. UV–vis spectrophotometric characterization of the isolated compounds was accomplished.

## 3. Results and discussion

### 3.1. *MALDI-TOF mass spectrometry of 1, 2, and 3*

The purity of synthesized complexes is additionally checked by laser desorption and ionization time-of-flight (LDI-TOF) mass spectrometry without matrix assistance or in the presence of 2,5-DHB as matrix (matrix-assisted LDI-TOF mass spectrometry, MALDI-TOF MS). In general, the LDI spectra of complexes synthesized in this work do not contain signals derived from ligands alone, suggesting high stability of the metal–ligand bond. Usually, ions detectable in the spectra of transition metal complexes are generated by the loss of anions, or loss of one or more ligands [27]. Some signals can be, however, generated by the addition of the other ions, such as $OH^-$ or $Cl^-$ or, in some cases, $H_2O$ or another ligand.

The positive ion LDI-TOF mass spectrum of **1** shows signal at *m/z* = 760.8 is derived from loss of one $ClO_4^-$ (figure S2). One should keep in mind that all signals that arise from Pt-containing ions represent actually a group of signals due to high number or Pt-isotopes. The other signal observed at *m/z* = 315.3 represents a positive ion assigned to the cluster $[[Pt(en)] + (en)]^+$, while the signal at *m/z* = 370.7 can be ascribed to $[Pt(en)(pz)Cl]^+$.

The positive ion LDI-TOF mass spectrum of **2** shows a signal at *m/z* = 860.9 after loss of one $ClO_4^-$ (figure S3), while the ions formed after the loss of both $ClO_4^-$ anions are at *m/z* = 761.5. The signal at *m/z* = 681.4 stems from the cluster generated from two $[Pt(dach)Cl]^+$ fragments. Another signal of medium intensity at *m/z* = 420.8 is ascribed to the positive ion $[Pt(dach)(pz)Cl]^+$, while the signal with the highest intensity occurs at *m/z* = 385.3 due to $[Pt(dach)(pz)]^{\cdot+}$. As an illustration, the positive ion MALDI-TOF mass spectrum of **3** is given in figure S3. There is a signal at *m/z* = 937.1 after loss of one $ClO_4^-$, while the ions formed after the loss of both $ClO_4^-$ anions appear at *m/z* = 837.6. The most intense signal is detectable at *m/z* = 496.9 and is derived from **3** after loss of one $[Pt(dach)Cl]^+$ fragment and $ClO_4^-$. Table 1 summarizes all results obtained from mass spectrometry measurements.

### 3.2. *Determination of the p$K_a$ values of 1a, 2a, and 3a*

Figure 3 shows a typical example of the spectral changes observed during a pH titration of **3a** (see figures S5 and S6 for corresponding data of **1a** and **2a**, respectively). The titration data for the complexes were fitted for the determination of both p$K_a$ values [16] and the obtained data are presented in table 2.

The p$K_a$ value of coordinated water at Pt(II) is a good indicator of the electrophilicity of the metal center [14, 24, 25, 28]. For all complexes, two p$K_a$ values were obtained (table 2). The p$K_a$ values of **1a** are lower compared to **2a**. These complexes contain the

Table 1. Peaks detected in the positive ion LDI-TOF and MALDI-TOF mass spectra of **1**, **2**, and **3**.

| Peak position *(m/z)* | *m/z* range | Peak assignment |
|---|---|---|
| For **1** | | |
| 315.3 | 312.1–320.1 | $[[Pt(en)] + (en)]^+$ |
| 370.7 | 367.0–377.0 | $[Pt(en)(pz)Cl]^+$ |
| 760.8 | 754.9–767.9 | $[Pt_2(en)_2(pz)Cl_2]ClO_4^+$ |
| For **2** | | |
| 385.3 | 382.1–391.1 | $[Pt(dach)(pz)]\cdot^+$ |
| 420.8 | 417.1–427.1 | $[Pt(dach)(pz)Cl]^+$ |
| 681.4 | 676.0–689.0 | $2[Pt(dach)Cl]^+$ |
| 761.5 | 756.1–769.1 | $[Pt_2(dach)_2(pz)Cl_2]\cdot^+$ |
| 860.9 | 855.0–868.0 | $[Pt_2(dach)_2(pz)Cl_2]ClO_4^+$ |
| For **3** | | |
| 461.4 | 458.1–467.1 | $[Pt(dach)(4,4'\text{-bipy})]\cdot^+$ |
| 496.9 | 493.1–503.1 | $[Pt(dach)(4,4'\text{-bipy})Cl]^+$ |
| 837.6 | 832.1–845.1 | $[Pt_2(dach)_2(4,4'\text{-bipy})Cl_2]\cdot^+$ |
| 937.1 | 934.1–945.1 | $[Pt_2(dach)_2(4,4'\text{-bipy})Cl_2]ClO_4^+$ |

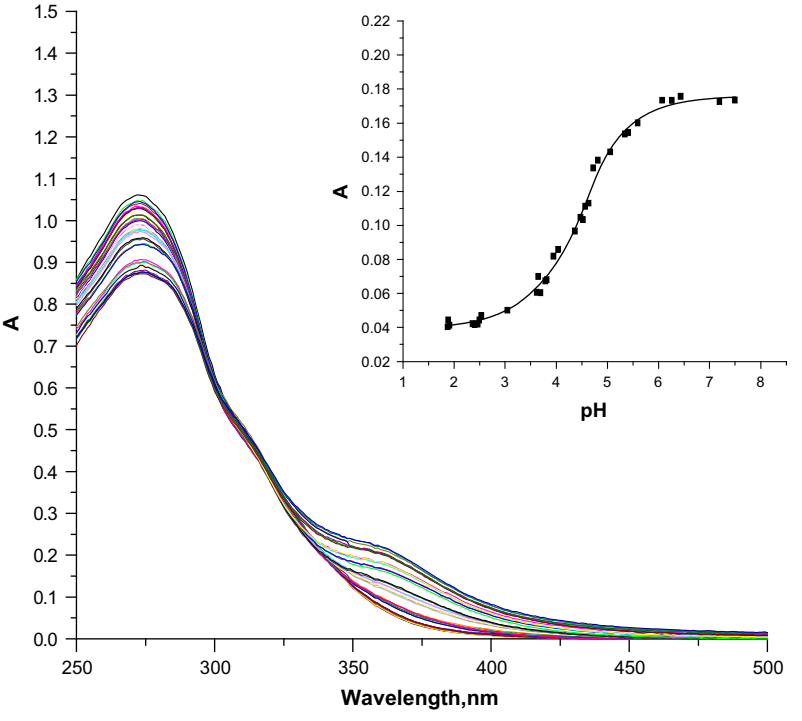


Figure 3. UV–vis spectra of **3a** recorded as a function of pH from 2 to 10 at $I = 0.01$ mol $L^{-1}$ $NaClO_4$ and 298 K. Insert graph: titration curve at 360 nm.

Table 2. Summary of p$K_a$ values of the diaqua complexes.

| Complex | p$K_{a1}$ | p$K_{a2}$ | Reference |
|---|---|---|---|
| **1a** | 4.32 ± 0.05 | 5.2 ± 0.2 | This work |
| **2a** | 4.48 ± 0.10 | 5.53 ± 0.05 | This work |
| **3a** | 4.65 ± 0.05 | 5.75 ± 0.20 | This work |
| $[\{Pt(dach)(H_2O)\}_2(\mu\text{-}NH_2(CH_2)_8NH_2)]^{4+}$ | 5.71 | – | [15] |
| $[\{Pt(dach)(H_2O)\}_2(\mu\text{-}NH_2(CH_2)_{10}NH_2)]^{4+}$ | 5.60 | – | [15] |

same bridging ligand (pz), so the difference in p$K_a$ values is affected by the nature of inert ligands (en in **1a** and dach in **2a**). This is in agreement with the fact that increasing of the $\sigma$-donor capacity of ligand leads to a higher p$K_a$ value, which reflects the reduced electrophilicity of the metal center and leads to a less reactive metal center [21b]. The obtained p$K_a$ values of **1a** and **2a** are lower than for **3a**. This could be associated with shorter distance between two Pt(II) centers (in the case of **1a** and **2a**) and with π-acceptor ability of the pyrazine ligand, by which the metal centers in **1a** and **2a** become more electrophilic and then more acidic [28, 29]. It is known from earlier studies that water ligands coordinated to each platinum center can exhibit different p$K_a$ values depending on the distance between the two metal centers. In table 2, p$K_a$ values of some dinuclear Pt(II) complexes containing dach as an inert ligand and diaminoalkane with eight or ten $CH_2$ units as bridging ligand are shown [15]. From table 2, it can be seen that dinuclear Pt(II) complexes with eight or ten $CH_2$ units as bridging ligand show only one p$K_a$ value. Metal centers in both these complexes are so far apart that any possible electronic communication between them can be ruled out. The p$K_a$ values of mononuclear complexes (p$K_{a1}$ = 5.97; p$K_{a2}$ = 7.47 for $[Pt(en)(H_2O)_2]^{2+}$ and p$K_{a1}$ = 6.01; p$K_{a2}$ = 7.69 for $[Pt(dach)(H_2O)_2]^{2+}$) [21b] are higher than p$K_a$ values for the dinuclear Pt(II) complexes studied in this work. We believe that this can be related to π-acceptor ability of the bridging ligands, making the metal centers more electrophilic and then more acidic [15, 28, 29]. The other reason is that a shorter distance between the platinum ions of dinuclear complexes results in the addition of single charges of the platinum centers, causing each platinum ion to become more electrophilic and acidic.

Based on the presented results in table 2, higher p$K_{a2}$ values compared to the p$K_{a1}$ for all studied dinuclear Pt(II) complexes are observed. After deprotonation of the first water, charge of the complex is reduced to +3 causing smaller amount of charge assigned to each platinum ion and as a result electrophilicity of the platinum ions is reduced and the acidity of the second water molecule is lower [14, 16].

### 3.3. *Kinetic measurements*

Substitution reactions of dinuclear Pt(II) complexes with nitrogen-bonding ligands were investigated spectrophotometrically by following the change in absorbance at suitable wavelengths as a function of time at 310 K. The reactions with the diaqua complexes were performed at pH 2.5 (0.01 mol $L^{-1}$ $NaClO_4$), while the reactions of the corresponding dichloride complexes were studied at pH 7.2 (25 mmol $L^{-1}$ Hepes buffer) in the presence of 40 mmol $L^{-1}$ NaCl in order to suppress spontaneous hydrolysis of the complexes. All kinetic traces gave an excellent fit to a double exponential function, typical for a two-step reaction.

The obtained *pseudo*-first-order rate constants, $k_{obsd1}$ and $k_{obsd2}$, calculated from the kinetic traces were plotted against the concentration of the entering ligands. A linear dependence on the nucleophile concentration was obtained for all the studied reactions (see figures 4, S7 and S8). The proposed reaction pathways for all substitution processes of the complexes are presented in scheme 1.

### 3.4. *Reactions of 1a, 2a, and 3a*

Substitution reactions of the diaqua complexes were studied at pH 2.5 (0.01 mol $L^{-1}$ $NaClO_4$). At this pH, the aqua complexes exist in diaqua form, based on the p$K_a$ values (table 2). The substitution reactions of the studied dinuclear Pt(II) complexes with the selected nucleophiles occur in two subsequent reversible steps (scheme 1). The first step represents substitution of labile water from the coordination sphere of the dinuclear Pt(II) complex by the nucleophile. This step is characterized by the rate constant $k_1$ for direct substitution and $k_{-1}$ for the anation. The second step is substitution of another labile water, where $k_2$ is marked as a rate constant for forward reaction and with $k_{-2}$ rate constant for the anation.

The dependence of the observed *pseudo*-first-order rate constants, $k_{obsd1}$ and $k_{obsd2}$, on the concentration of the entering ligands can be presented by equations (1) and (2). The second-order rate constants, $k_1$ and $k_2$, are calculated from the slope of the observed straight lines, while the rate constants, $k_{-1}$ and $k_{-2}$, are determined from the intercept. All kinetic data are summarized in tables S1–S6 (Supplementa1 data).

$$k_{obsd1} = k_{-1} + k_1[L] \quad (1)$$

$$k_{obsd2} = k_{-2} + k_2[L] \quad (2)$$

The obtained results for both reaction steps are summarized in table 3.

The order of the reactivity of investigated diaqua complexes for the first and second reaction steps is: **1a** > **2a** > **3a**. **1a** and **2a** have the same bridging ligand (pyrazine) and the difference in reactivity between these complexes can be ascribed to coordination geometry of the inert ligands (en and dach). Complex **2a** with dach as inert ligand has more steric hindrance and it is harder for entering ligands to approach the metal centers. The other possible reason for lower reactivity of **2a** in both reaction steps is less electrophilicity of the Pt(II) centers caused by the positive inductive effect of the cyclohexane ring [21b, 30].

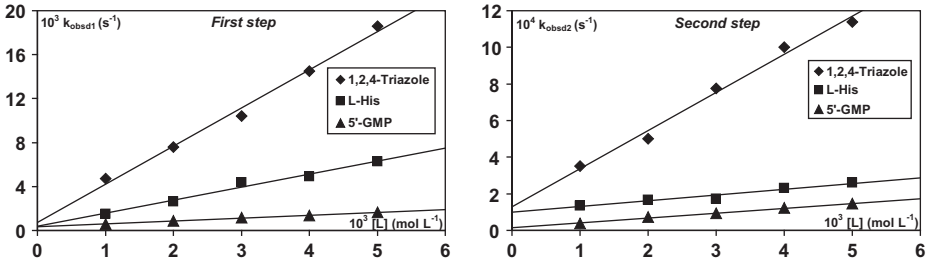


Figure 4. *Pseudo*-first-order rate constants plotted as a function of nucleophile concentration for the first and second substitution reactions of **1a** by 1,2,4-triazole, L-His, and 5′-GMP at pH 2.5 in 0.01 mol $L^{-1}$ $NaClO_4$ and 310 K.

Complexes containing pyrazine as bridging ligand, **1a** and **2a**, react about two times faster than **3a**. All three complexes include bridging ligands with π-acceptor ability, increasing electrophilicity of the platinum centers, and the reactivity of the complexes toward nucleophiles. The reason for the faster reactions of **1a** and **2a** is the short distance between the two metal centers, which involves electrostatic interactions between them [16]. The metal centers in **1a** and **2a** become more electrophilic and favor rapid binding of the entering nucleophile. Therefore, due to nature of bridging ligand in **3a**, the distance between two metal centers is longer, leading to lower electron communication between platinum centers, and then to decreasing electrophilicity, causing the lower reactivity of **3a** compared to the other studied complexes.

The order of reactivity for both substitution steps is: 1,2,4-triazole > L-His > 5′-GMP (table 3). 1,2,4-Triazole is the most reactive nucleophile because of steric effect. 1,2,4-Triazole is less crowded and can approach the Pt(II) center in the easiest way. However, the difference between the triazole and imidazole rings (L-His) is that triazole is a five-membered ring with three conjugated nitrogens, which makes triazole very electron rich and a good nucleophile. Imidazole in the L-His is also a five-membered ring with two conjugated nitrogens, less electron rich and weaker compared to triazole. The lowest reactivity of 5′-GMP can be related to the steric effects of this ligand.

Higher values of $k_1$ than $k_2$ are obtained in all studied systems (table 3). After coordination of the first nucleophile, the approach of the second is more difficult because of steric hindrance and the rate constants which were obtained have lower values.

### 3.5. *Reactions of 1, 2, and 3*

The substitution reactions of the dichloride dinuclear Pt(II) complexes occur in two reaction steps determined by two second-order rate constants $k_1$ and $k_2$ (scheme 1); these values are presented in table 4.

Substitution reactions of square-planar metal complexes can proceed through to two parallel pathways [31]. One involves the formation of a solvent-coordinated complex, followed by rapid substitution of the coordinated solvent by the entering nucleophile (solvolytic pathway), and the other involves direct nucleophilic attack by the entering nucleophile. The solvolytic pathway was suppressed through addition of 40 mmol $L^{-1}$ NaCl and as such the reaction goes to equilibrium (scheme 1). Under *pseudo*-first-order conditions, these rate constants can be determined from a plot of the linear dependence of $k_{obsd}$ *versus* the total nucleophile concentration, according to equations (3) and (4). The slope of the line represents $k_1$ or $k_2$, whereas the intercept represents $k_{-1}[Cl^-]$ or $k_{-2}[Cl^-]$. All kinetic data are summarized in tables S7–S12 (Supplementa1 data).

The observed *pseudo*-first-order rate constants, $k_{obsd1}$ and $k_{obsd2}$, as a function of the total concentration of nucleophile are described by equations (3) and (4).

$$k_{obsd1} = k_{-1}[Cl^-] + k_1[L] \quad (3)$$

$$k_{obsd2} = k_{-2}[Cl^-] + k_2[L] \quad (4)$$

The reactivity of the nucleophiles toward all complexes follows the same order as at pH 2.5, 1,2,4-triazole > L-His > 5′-GMP. Comparing the obtained results for $k_1$ and $k_2$ in tables 3 and 4 the dichloride complexes are less reactive than their diaqua analogs, due to the stronger Pt–Cl bonds [6, 16].

Table 3. Rate constants for the first and the second step of the reactions of **1a**, **2a,** and **3a** with 1,2,4-triazole, L-His, and 5′-GMP at pH 2.5 (0.01 mol $L^{-1}$ $NaClO_4$) and 310 K.

| | First step | | Second step | |
|---|---|---|---|---|
| | $10^2$ $k_1$[$M^{-1}$ $s^{-1}$] | $10^2 k_{-1}$[$s^{-1}$] | $10^2$ $k_2$[$M^{-1}$ $s^{-1}$] | $10^2$ $k_{-2}$[$s^{-1}$] |
| Complex **1a** | | | | |
| 1,2,4-Triazole | 347 ± 20 | 0.073 ± 0.006 | 20.8 ± 0.9 | 0.013 ± 0.004 |
| L-His | 119 ± 9 | 0.039 ± 0.005 | 3.2 ± 0.5 | 0.009 ± 0.001 |
| 5′-GMP | 25.9 ± 0.9 | 0.035 ± 0.005 | 2.6 ± 0.5 | 0.002 ± 0.001 |
| Complex **2a** | | | | |
| 1,2,4-Triazole | 319 ± 30 | 0.051 ± 0.001 | 18.7 ± 0.5 | 0.007 ± 0.001 |
| L-His | 105 ± 9 | 0.013 ± 0.001 | 2.5 ± 0.1 | 0.005 ± 0.001 |
| 5′-GMP | 21.2 ± 0.5 | 0.028 ± 0.005 | 1.5 ± 0.1 | 0.002 ± 0.001 |
| Complex **3a** | | | | |
| 1,2,4-Triazole | 154 ± 6 | 0.05 ± 0.02 | 10.76 ± 0.05 | 0.004 ± 0.001 |
| L-His | 56 ± 3 | 0.02 ± 0.01 | 1.4 ± 0.1 | 0.003 ± 0.001 |
| 5′-GMP | 14 ± 2 | 0.005 ± 0.001 | 1.32 ± 0.01 | 0.002 ± 0.001 |

Table 4. Rate constants for the first and second step of the reactions of **1**, **2,** and **3** with 1,2,4-triazole, L-His, and 5′-GMP at pH 7.2 (25 mmol $L^{-1}$ Hepes buffer) in the presence of 40 mmol $L^{-1}$ NaCl at 310 K.

| | First step | | Second step | |
|---|---|---|---|---|
| | $10^2$ $k_1$[$M^{-1}$ $s^{-1}$] | $10^2$ $k_{-1}$[$M^{-1}$ $s^{-1}$][b] | $10^2$ $k_2$[$M^{-1}$ $s^{-1}$] | $10^2$ $k_{-2}$[$M^{-1}$ $s^{-1}$][b] |
| Complex **1** | | | | |
| 1,2,4-Triazole | 70 ± 5 | 2.7 ± 0.5 | 1.47 ± 0.09 | 0.015 ± 0.008 |
| L-His | 9.8 ± 0.9 | 0.50 ± 0.07 | 0.96 ± 0.01 | 0.015 ± 0.002 |
| 5′-GMP | 5.8 ± 0.3 | 0.15 ± 0.02 | 0.90 ± 0.07 | 0.007 ± 0.002 |
| 5′-GMP[a] | 1.60 ± 0.02 | | | |
| Complex **2** | | | | |
| 1,2,4-Triazole | 67 ± 4 | 1.8 ± 0.3 | 1.3 ± 0.1 | 0.015 ± 0.007 |
| L-His | 9.1 ± 0.9 | 0.50 ± 0.07 | 0.94 ± 0.01 | 0.007 ± 0.002 |
| 5′-GMP | 5.4 ± 0.2 | 0.10 ± 0.02 | 0.68 ± 0.06 | 0.012 ± 0.002 |
| 5′-GMP[a] | 1.14 ± 0.01 | | | |
| Complex **3** | | | | |
| 1,2,4-Triazole | 56 ± 5 | 1.45 ± 0.05 | 0.76 ± 0.01 | 0.020 ± 0.002 |
| L-His | 7.7 ± 0.6 | 0.25 ± 0.02 | 0.57 ± 0.06 | 0.012 ± 0.003 |
| 5′-GMP | 4.7 ± 0.5 | 0.05 ± 0.02 | 0.46 ± 0.04 | 0.010 ± 0.002 |

[a]Rate constant obtained by NMR experiments, pD = 6.7 and 295 K.
[b]Calculated from $k_{-1}[Cl^-]$ and $k_{-2}[Cl^-]$ since $[Cl^-] = 40$ mmol $L^{-1}$.

1,2,4-Triazole shows the highest reactivity from all studied nucleophiles toward selected dinuclear complexes; 5′-GMP is sterically more crowded than 1,2,4-triazole and L-His and reacts slower. The reasons for the observed order of the reactivity are the same as has been described for the diaqua complexes.

The order of reactivity of the investigated dichloride Pt(II) complexes is also the same as for diaqua analogs, **1** > **2** > **3**. The rate constants $k_{-1}$ and $k_{-2}$, which are independent of nucleophile concentration, are much smaller than $k_1$ and $k_2$ and contribute little to the observed rate. The explanation for the resulting order of the reactivity of the complexes is given in the previous section.

The activation parameters ($\Delta H^{\neq}$ and $\Delta S^{\neq}$) for reactions with 5′-GMP at pH 2.5 and 7.2 were calculated using the Eyring equation and are summarized in tables S13 and S14 (Supplemental data). Activation parameters support an associative mechanism for all reactions. The value of the activation entropy of the second substitution step has been always more negative than the value for the first step, which indicates weaker molecular interactions and confirms slower second reaction step [13].

### 3.6. *$^1$H NMR measurements*

The kinetics of the substitution reactions of **1**, **2,** and **3** with 5′-GMP in $D_2O$ at pD 6.7 and 295 K were studied by $^1$H NMR spectroscopy under second-order conditions with an initial molar ratio of 1 : 1. Second-order rate constants for **1** and **2** were obtained from equation (5) [32],

$$k_1 t = \frac{x}{a_0(a_0 - x)} \tag{5}$$

where $x$ is the amount of coordinated 5′-GMP and $a_0$ is the initial concentration of free ligand. The concentration $x$ is calculated considering the area of the signals for free and coordinated 5′-GMP. The value of the rate constant was determined from a Guggenheim plot [32] in which $x/a_0(a_0 - x)$ is plotted against time. The slope of the straight line, which passes through zero, represents the value of the rate constant $k_1$, as shown in figures S9 and S10 for **1** and **2**, respectively.

The addition of 5′-GMP (1 eq.) to the solution of **1** (1 eq.) in $D_2O$ induced changes in the $^1$H NMR spectrum (figure 5). New resonances attributed to [{Pt(en)Cl}($\mu$-pz){Pt(en)

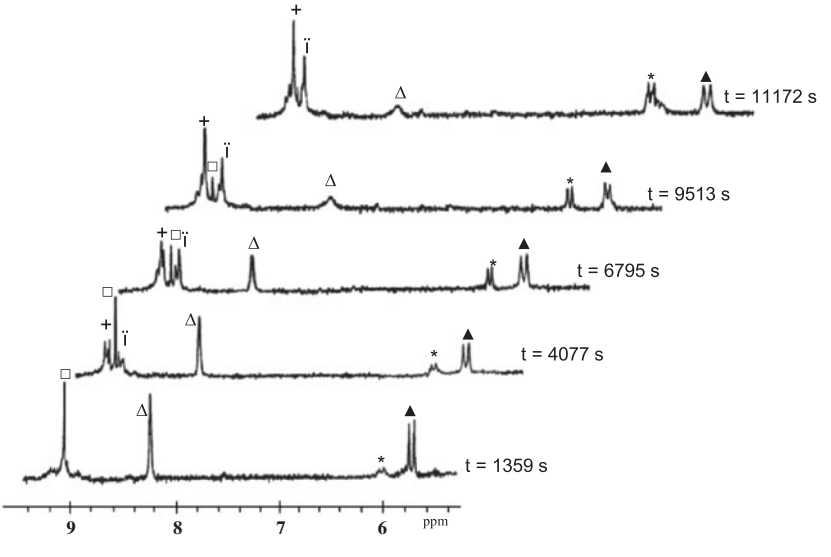


Figure 5. $^1$H NMR spectra of the reaction between **1** and 5′-GMP in molar ratio 1 : 1 where (Δ) is H8 signal of free 5′-GMP, (•) is H8 signal of coordinated 5′-GMP, (□) is signal of CH pyrazine of free complex, (+) is signal of CH pyrazine in the product, (*) is H1′ signal of coordinated 5′-GMP, and (▲) is H1′ signal of free 5′-GMP at pD 6.7 and 295 K.

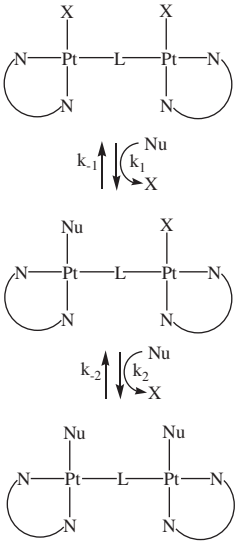


X = $H_2O$, $Cl^-$; Nu = 1,2,4-triazole, L-His, 5'-GMP

L = pyrazine, 4,4'-bipyridyl; N-**N = en, dach**

Scheme 1.

(*N7-5′*-GMP)}]$^+$ started to appear after 22 min (figure 5). The coordination of 5′-GMP to Pt (II) occurs, as seen from the signal of H1′ proton of 5′-GMP moving from 5.84 ppm (free 5′-GMP) to 6.04 ppm. Increase in the intensity of the doublet at the 6.04 ppm and decreasing intensity of the doublet at 5.84 ppm supports product formation. The spectrum after 3 h shows that around half of starting 5′-GMP is coordinated, according to the intensity of doublets (5.84 and 6.04 ppm).

The coordinations of 5′-GMP to **2** and **3** are presented in figures S11 and S12. In both reactions, concentration of the free 5′-GMP decreases while the concentration for coordinated 5′-GMP increases, according to the intensity of the H1′ protons. The equilibrium was established after a few hours and the chloride was substituted by 5′-GMP.

The H8 from 5′-GMP appears in the spectrum of **1** and **2** as a singlet and decreases in intensity during time (figures 5 and S11). The area around 9 ppm during reactions has several signals; we observe that the singlet originating from pyrazine of the complex decreases over time (figures 5 and S11). Because there was a multiplicity of signals in this area, it was impossible to take the integrals of the H8 protons (5′-GMP) for determination of the rate constant, and we therefore used the intensity of the doublet of the H1′ proton of 5′-GMP. In the spectrum of **3** in the area around 8 and 9 ppm, only free and coordinated protons of $CH_\beta$4-pyridine and $CH_\alpha$4-pyridine as multiplets are observed. The calculated values of $k_1$ are presented in table 4.

### 3.7. *HPLC measurements*

Substitution of the chloride in **1**, **2**, and **3** with 5′-GMP were monitored by HPLC. The thermostated solution (310 K), obtained by mixing the solution of the complexes and ligand in

the molar ratio 1 : 2, was injected at different time intervals. The obtained HPLC chromatograms for all three complexes are shown in figures S13, S14, and S15.

From figures S13, S14, and S15 after half an hour of mixing complex and ligand, chromatograms present three different peaks. These peaks can be attributed to starting complexes (**1** retention time 3.2 min; **2** retention time 2.2 min; **3** retention time 2.8 min), free 5′-GMP, (**1** retention time 2.5 min; **2** retention time 2.0 min; **3** retention time 2.0 min), and small peak that belongs to the product (**1** retention time 2.2 min; **2** retention time 2.5 min; **3** retention time 2.5 min). During the reactions, we observe that the peaks of the complex and the free ligand decrease, while the peaks of the products grow. After 72 h, only one peak is observed in the chromatograms for all three complexes. This peak belongs to the product of the reactions in which both chlorides are substituted with 5′-GMP as no signal of free 5′-GMP or complex were observed. The starting ratio between complexes and 5′-GMP was 1 : 2 and no signal of free 5′-GMP was observed in chromatograms of the end of the reaction. We conclude that both 5′-GMP molecules are coordinated to Pt(II). Decomposition of the starting complex was not observed as we did not observe any new peaks in the chromatograms.



## 4. Conclusion

The substitution reactions of dinuclear Pt(II) complexes with selected N-bonding nucleophiles were investigated. The studied substitution reactions occur in two subsequent steps. These dinuclear Pt(II) complexes have a high affinity for the N-donor ligands of which 1,2,4-triazole is a better nucleophile than L-His and 5′-GMP. The order of the reactivity is: **1** > **2** > **3**. The nature of bridging ligand as well as the nature of the inert ligand plays an important role in the kinetic behavior of the dinuclear Pt(II) complexes. The studied bridging ligands are π-acceptors so they increase the electrophilicity on Pt(II), due to their electron-withdrawing properties, which results in increasing rates of nucleophilic substitution reactions. This effect is strongest for pyrazine as bridging ligand. For all complexes it was possible to determinate two p$K_a$ values. The increase in electrophilicity of the platinum centers leads to decreases of the p$K_a$ values. The mechanism of the substitution reactions is associative, supported by the negative values of $\Delta S^{\neq}$ for both substitution steps.

The obtained results show that the reactivity and p$K_a$ values of dinuclear Pt(II) complexes can be changed by modifying the properties of their bridging and inert ligands. Finally, these results could contribute to better understanding of the interactions of dinuclear Pt(II) complexes with biologically important nucleophiles, such as constituents of DNA, peptides, and proteins.

## Acknowledgements

The authors gratefully acknowledge financial support of the Ministry of Education, Science and Technological Development, Republic of Serbia (Project No. 172011).

## Disclosure statement

No potential conflict of interest was reported by the authors.

## References


[1] B. Lippert (Ed.). *Cisplatin: Chemistry and Biochemistry of a Leading Anticancer Drug*, Wiley-VCH, Zürich (1999).
[2] E. Alessio. *Bioinorganic Medicinal Chemistry*, Wiley-VCH, Weinheim (2011).
[3] N.P.E. Barry, P.J. Sadler. *Chem. Commun.*, **49**, 5106 (2013).
[4] L. Ronconi, P.J. Sadler. *Coord. Chem. Rev.*, **251**, 1633 (2007).
[5] M.A. Jakupec, M. Galanski, V.B. Arion, C.G. Hartinger, B.K. Keppler. *Dalton Trans.*, **2**, 183 (2008).
[6] Ž.D. Bugarčić, J. Bogojeski, B. Petrović, S. Hochreuther, R. van Eldik. *Dalton Trans.*, **41**, 12329 (2012).
[7] N. Farrell. *Comments Inorg. Chem.*, **16**, 373 (1995).
[8] V. Brabec, J. Kašpárková, O. Vrána, O. Nováková, J.W. Cox, Y. Qu, N. Farrell. *Biochemistry*, **38**, 6781 (1999).
[9] Y. Qu, N. Farrell. *J. Am. Chem. Soc.*, **113**, 4851 (1991).
[10] J.W. Cox, S.J. Berners-Price, M.S. Davies, Y. Qu, N. Farrell. *J. Am. Chem. Soc.*, **123**, 1316 (2001).
[11] V. Brabec, J. Kasparkova. *Drug Resist. Updates*, **8**, 131 (2005).
[12] (a) N. Farrell, Y. Qu. *Inorg. Chem.*, **28**, 3416 (1989); (b) N. Farrell, S.G. de Almeida, K.A. Skov. *J. Am. Chem. Soc.*, **110**, 5018 (1988); (c) N. Farrell, Y. Qu, M.P. Hacker. *J. Med. Chem.*, **33**, 2179 (1990); (d) J.D. Roberts, B. van Houten, Y. Qu, N.P. Farrell. *Nucleic Acids Res.*, **17**, 9719 (1989); (e) A. Kraker, W. Elliott, B. van Houten, N. Farrell, J. Hoeschele, J. Roberts. *J. Inorg. Biochem.*, **36**, 160 (1989).
[13] S. Hochreuther, R. Puchta, R. van Eldik. *Inorg. Chem.*, **50**, 8984 (2011).
[14] H. Ertürk, A. Hofmann, R. Puchta, R. van Eldik. *Dalton Trans.*, **22**, 2295 (2007).
[15] H. Ertürk, R. Puchta, R. van Eldik. *Eur. J. Inorg. Chem.*, **10**, 1331 (2009).
[16] T. Soldatović, S. Jovanović, Ž.D. Bugarčić, R. van Eldik. *Dalton Trans.*, **41**, 876 (2012).
[17] D. Jaganyi, V.M. Munisamy, D. Reddy. *Int. J. Chem. Kinet.*, **38**, 202 (2006).
[18] P.O. Ongoma, D. Jaganyi. *Transition Met. Chem.*, **38**, 587 (2013).
[19] S.M. Saini, J. Dwivedi. *Int. J. Pharm. Sci. Res.*, **4**, 2866 (2013).
[20] W. Kaim, B. Schwederski, A. Klein. *Bioinorganic Chemistry: Inorganic Elements in the Chemistry of Life*, 2nd Edn, pp. 99–114, Wiley, Chichester (2013).
[21] (a) B.A. Howell, R. Rashidianfar, J.R. Glass, B.J. Hutchinson, D.A. Johnson. *Inorg. Chim. Acta*, **142**, 181 (1988); (b) N. Summa, W. Schiessl, R. Puchta, N. van Eikema Hommes, R. van Eldik. *Inorg. Chem.*, **45**, 2948 (2006).
[22] S. Rajković, D.P. Ašanin, M.D. Živković, M.I. Djuran. *Polyhedron*, **65**, 42 (2013).
[23] S. Komeda, G.V. Kalayda, M. Lutz, A.L. Spek, Y. Yamanaka, T. Sato, M. Chikuma, J. Reedijk. *J. Med. Chem.*, **46**, 1210 (2003).
[24] D. Jaganyi, A. Hofmann, R. van Eldik. *Angew. Chem.*, **40**, 1680 (2001).
[25] A. Hofmann, D. Jaganyi, O.Q. Munro, G. Liehr, R. van Eldik. *Inorg. Chem.*, **42**, 1688 (2003).
[26] K. Mikkelsen, S.O. Nielsen. *J. Phys. Chem.*, **64**, 632 (1960).
[27] M. Radisavljević, T. Kamčeva, I. Vukićević, M. Radoičić, Z. Šaponjić, M. Petković. *Rapid Commun. Mass Spectrom.*, **26**, 2041 (2012).
[28] A. Hofmann, R. van Eldik. *Dalton Trans.*, **15**, 2979 (2003).
[29] D. Reddy, D. Jaganyi. *Int. J. Chem. Kinet.*, **43**, 161 (2011).
[30] S. Jovanović, B. Petrović, D. Čanović, Ž.D. Bugarčić. *Int. J. Chem. Kinet.*, **43**, 99 (2011).
[31] M.L. Tobe, J. Burgess. *Inorganic Reaction Mechanisms*, Addison Wesley Longman Inc., Essex (1999).
[32] S.K. Upadhyay. *Chemical Kinetics and Reaction Dynamics*, 6th Edn, Springer, New York (2006).